ChemPubSoc Europe

DOI: 10.1002/ejic.201700430

EurJIC European Journal of Inorganic Chemistry

Full Paper

Cage Compounds

# Potassium and Yttrium Complexes of a Rigid Bis-Phosphido POP-Donor Ligand

Kelly S. A. Motolko,[a] David J. H. Emslie*[a] Hilary A. Jenkins,[b] and James F. Britten[b]

**Abstract:** Dilithiation of 4,5-dibromo-2,7-di-*tert*-butyl-9,9-dimethyl-xanthene ($XBr_2$) followed by addition of 2 equiv. of (2,4,6-triisopropylphenyl)dichlorophosphine ($TrippPCl_2$) afforded 4,5-bis[(2,4,6-triisopropylphenyl)chlorophosphino]-2,7-di-*tert*-butyl-9,9-dimethylxanthene ($XP_2Cl_2$), which was reduced to 4,5-bis[(2,4,6-triisopropylphenyl)phosphino]-2,7-di-*tert*-butyl-9,9-dimethylxanthene ($H_2XP_2$) using excess $LiAlH_4$. Deprotonation of $H_2XP_2$ with excess KH in DME provided the dipotassium salt, $[K_2(XP_2)(dme)_n]$ (**1**; $n$ = 2.5–4), and stirring **1** in THF followed by recrystallization from hexanes yielded tetrametallic $[K_4(XP_2)_2(THF)_4]$ (**2**) which features a central $K_4P_4$ cage. Reaction of $[YI_3(THF)_{3.5}]$ with $[K_2XP_2(dme)_{2.5}]$ afforded a mixture of products including $[(XP_2)YI(THF)_2]$ (**3**) and $(PTripp)_3$; pure **3** could be isolated in low yield by extraction with a minimum volume of hexanes or $O(SiMe_3)_2$. In the solid state, **3** adopts a face-capped trigonal bipyramidal coordination geometry with a planar xanthene backbone and an angle of 85° between the P(1)/C(4)/C(5)/P(2) and P(1)/Y/P(2) planes.

## Introduction

Ancillary ligands play a critical role in defining the thermal stability and reactivity of metal complexes, and we have previously explored the use of rigid 4,5-bis(anilido)xanthene ligands in actinide and lanthanide chemistry. For example, the $XA_2$ [4,5-bis(2,6-diisopropylanilido)-2,7-di-*tert*-butyl-9,9-dimethylxanthene] pincer ligand was employed for the synthesis of thorium(IV), uranium(IV) and uranium(III) chloro complexes,[1,2] as well as dialkyl complexes of tetravalent thorium[1,3] and uranium[4] (Figure 1), thorium(IV) monoalkyl cations, and a thorium(IV) dication.[3,5] Furthermore, we recently reported the synthesis of Y, Lu and La derivatives of the $XN_2$ [4,5-bis(2,4,6-triisopropylanilido)-2,7-di-*tert*-butyl-9,9-dimethylxanthene] ligand, including monoalkyl derivatives (Figure 1) which are highly active catalysts for alkene and alkyne hydroamination.[6,7]

In combination with large rare earth and actinide elements, the xanthene-backbone $XA_2$ and $XN_2$ ligands present a rigid meridionally-coordinating pincer array that is capable of stabilizing highly reactive organometallic derivatives. Additionally, the rigidity of the ligand framework provides an opportunity to introduce softer donor atoms into the coordination sphere of rare earth or actinide elements, and we have previously prepared uranium(III) and (IV) complexes of a thioxanthene analogue of the $XA_2$ ligand, $TXA_2$.[2] As an extension of this concept,

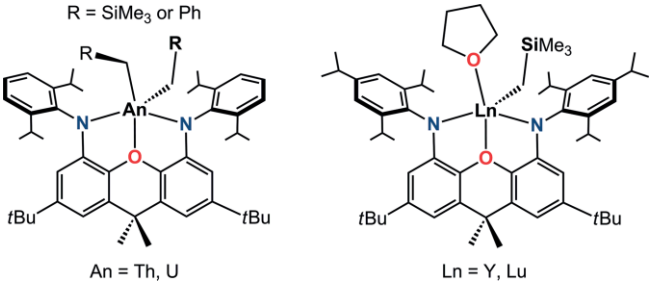


Figure 1. Neutral 4,5-bis(anilido)xanthene alkyl complexes of thorium(IV), uranium(IV), yttrium(III) and lutetium(III).

we became interested to probe the rare earth coordination behavior of a 4,5-bis(arylphosphido)xanthene analogue of $XN_2$.

In comparison to amido ligands, phosphido ligands are far less explored in group 3 and f-element chemistry,[8] especially multidentate ligands containing phosphido donors. Ligands of this type which have been employed in rare earth chemistry are illustrated in Figure 2. The PN-, PO-, PPP-, OPO- and Cp/P-donor ligands a,[9–11] b,[9,12] c (L = $PR_2$),[13] c (L = OMe),[14] and f[15,16] were assembled prior to metal coordination. By contrast, d[11,17] and g[16] resulted from cyclometallation, and dianionic e[12] formed from monoanionic b (R′ = H), through metal-mediated transfer of a methyl group from oxygen to the phosphorus donor of a second equivalent of ligand b.

Herein we report the synthesis of a direct phosphorus analogue of the $H_2[XN_2]$ pro-ligand, $H_2[XP_2]$, and potassium complexes of the $XP_2$ dianion, including the first example of a potassium phosphido compound with a $K_4P_4$ cubic cage structure. The synthesis and structural characterization of an yttrium iodido $XP_2$ complex is also described, allowing comparison of the binding preferences of $XP_2$ and $XN_2$ in the coordination sphere of yttrium.

[a] *Department of Chemistry & Chemical Biology, McMaster University, 1280 Main St. West, Hamilton, Ontario, L8S 4M1, Canada*
*E-mail: emslied@mcmaster.ca*
*http://www.chemistry.mcmaster.ca/emslie/emslie.html*
[b] *McMaster University Analytical X-ray Diffraction Facility, 1280 Main St. West, Hamilton, Ontario, L8S 4M1, Canada*
*Supporting information and ORCID(s) from the author(s) for this article are available on the WWW under https://doi.org/10.1002/ejic.201700430.*

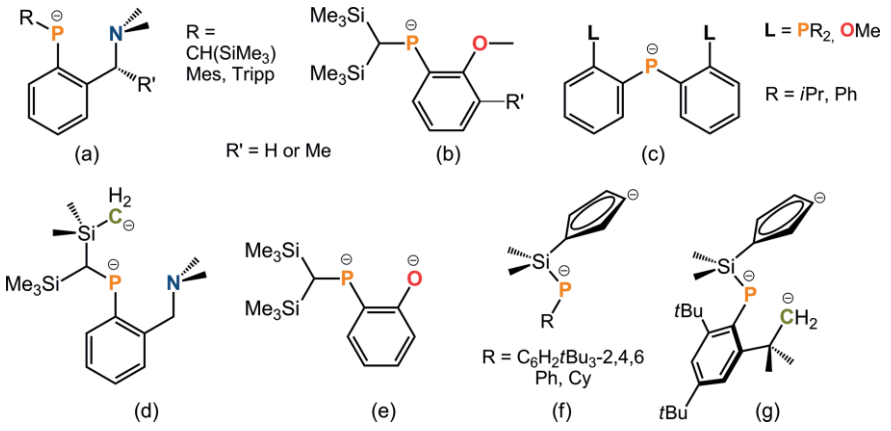


Figure 2. Multidentate phosphido ligands employed in rare earth chemistry.

## Results and Discussion

Reaction of 4,5-dibromo-2,7-di-*tert*-butyl-9,9-dimethylxanthene ($XBr_2$) with 2 equiv. of *n*BuLi in THF, followed by addition of 2 equiv. of (2,4,6-triisopropylphenyl)dichlorophosphine (Tripp-$PCl_2$) afforded a 73 % yield of 4,5-bis[(2,4,6-triisopropylphenyl)-chlorophosphino]-2,7-di-*tert*-butyl-9,9-dimethylxanthene ($XP_2Cl_2$) as an approximate 1:1 ratio of diastereomers (Scheme 1; diastereomers were not assigned as *rac* or *meso* due to overlapping $CMe_2$ signals in $^1H$ and $^{13}C$ NMR spectra of the $C_s$-symmetric *meso* isomer). Samples enriched in each diastereomer could be obtained by washing the isolated solid with a small volume of hexanes; the solid residue contained > 95 % of one diastereomer, while the mother liquor contained > 60 % of the other diastereomer.

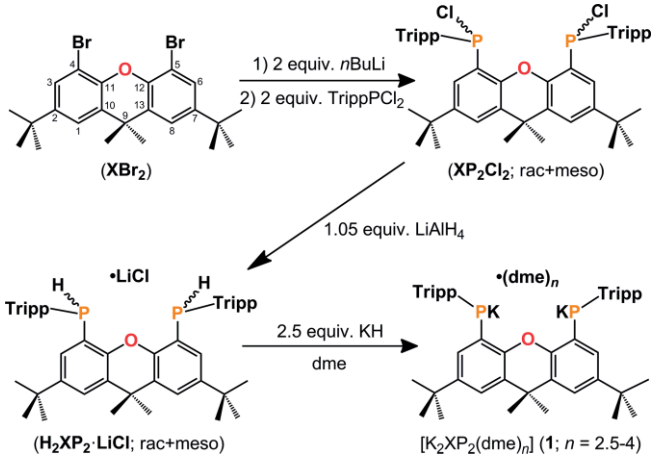


Scheme 1. Synthesis of $XP_2Cl_2$, $H_2XP_2$·LiCl and $[K_2(XP_2)(dme)_n]$ ($n$ = 2.5–4). Tripp = 2,4,6-triisopropylphenyl.

Pure or enriched samples of the diastereomers of $XP_2Cl_2$ were used to simplify NMR characterization. However, separation of diastereomers was not required prior to reaction with $LiAlH_4$ to form 4,5-bis[(2,4,6-triisopropylphenyl)phosphino]-2,7-di-*tert*-butyl-9,9-dimethyl-xanthene ($H_2XP_2$), which was isolated in 87 % yield as an approximate 1:1 mixture of diastereomers, containing 1.0–1.5 equiv. of occluded LiCl based on elemental analysis (Scheme 1). The $^1H$ and $^{31}P$ NMR spectra of $H_2XP_2$ revealed $^1J_{1H,31P}$ couplings of 225 Hz and 229 Hz for the P-H signals of the two diastereomers, similar to those in $Ph_2PH$ (218 Hz),[18] as well as related PCP-,[19] PNP-,[20] and POP-donor[21] pro-ligands (211–227 Hz).

Stirring $H_2XP_2$ with excess KH in DME for 72 h produced the dipotassium salt of the dianion, $[K_2(XP_2)(dme)_{2.5}]$ (**1**) as an orange solid in 80 % isolated yield (Scheme 1). The $^{31}P$ NMR spectrum of $[K_2(XP_2)(dme)_{2.5}]$ comprises of a single peak at $\delta$ = –83.7 ppm, consistent with the removal of chirality at phosphorus upon deprotonation, and the $^1H$ NMR spectrum is indicative of $C_{2v}$ symmetry. Crystals of $[K_2(XP_2)(dme)_4]$ were grown by cooling a concentrated DME solution to –30 °C (Figure 3) and reveal a $K_2P_2$ rhombus-shaped core, with 78–82° angles between the P(1)/C(4)/C(5)/P(2) and P(1)/K/P(2) planes. Two DME molecules are coordinated to each potassium atom and the ligand backbone is essentially planar with a 1° angle between the planes of the two aryl rings in the backbone.

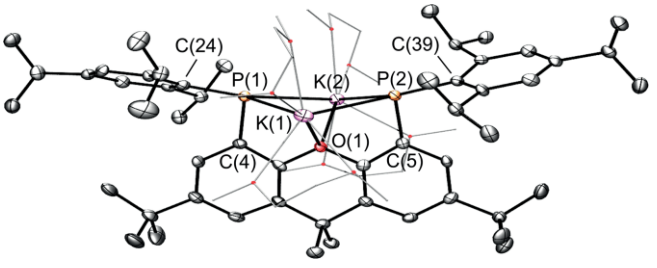


Figure 3. X-ray crystal structure of compound **1**. Ellipsoids are set at 50 % probability. The *tert*-butyl groups are rotationally disordered over multiple positions, and in each case, only one is shown for clarity. Hydrogen atoms are omitted, and the coordinating DME molecules are depicted in wire-frame. Selected bond lengths [Å] and angles [°]: K(1)–P(1) 3.395(2), K(1)–P(2) 3.332(1), K(2)–P(1) 3.320(1), K(2)–P(2) 3.277(1), K(1)–O(1) 2.868(3), K(2)–O(1) 2.958(2), P(1)–K(1)–P(2) 80.12(3), P(1)–K(2)–P(2) 82.03(3), K(1)–P(2)–K(2) 98.06(3), K(1)–P(1)–K(2) 96.00(3), C(4)–P(1)–C(24) 97.8(2), C(5)–P(2)–C(39) 100.6(2), K(1)–O(1)–K(2) 117.83(8), C(4)–P(1)–K(1) 84.2(1), C(4)–P(1)–K(2) 88.9(1), C(5)–P(2)–K(1) 85.5(1), C(5)–P(2)–K(2) 87.4(1), C(24)–P(1)–K(1) 134.1(1), C(24)–P(1)–K(2) 129.8(1), C(39)–P(2)–K(1) 130.2(1), C(39)–P(2)–K(2) 131.3(1).

Related phosphido complexes include polymeric $[\{K_2(POP)\}_\infty]$ [POP = 4,5-bis(*tert*-butylphosphido)-9,9-dimethyl-xanthene] fea-

turing K···P and K···$C_{aryl}$ contacts between adjacent $K_2$(POP) units,[21] [{(PNP)$K_2$(THF)$_3$}$_2$] {PNP = 2,6-bis[2-(phenylphosphido)-phenyl]pyridine} with a ladder-like $K_4P_4$ core,[20] and polymeric [{($Ph_2$P)K(pmdeta)}$_\infty$], and [{(RPhP)K(pmdeta)}$_2$] [R = CH(SiMe$_3$)$_2$; pmdeta = *N*,*N*′,*N*″,*N*‴-pentamethyldiethylene-triamine] with rhombus-shaped $K_2P_2$ cores.[22] The K–$O_{xant}$ distances of 2.868(3) and 2.958(2) Å in **1** are similar to those in $K_2$(POP) [2.869(2) Å], and the K–P distances in **1** [3.277(1) to 3.395(2) Å] fall within the range reported for the aforementioned literature compounds [3.128(1)–3.538(1) Å]. However, the C–P–C angles of 97.8(2) and 100.6(2)° are acute, more so than the compounds cited above [102.7(1)–107.5(1)°], presumably to minimize unfavorable steric interactions between *ortho*-isopropyl groups and the two dme ligands on each potassium centre.

Stirring [$K_2$($XP_2$)(dme)$_{2.5}$] (**1**) in THF at 24 °C for 5 h, followed by removal of the solvent in vacuo and recrystallization from hexanes afforded [$K_4$($XP_2$)$_2$(THF)$_4$] (**2**) as orange crystals in 22 % yield. The $^1$H NMR spectrum of **2** contains a single complement of peaks for a top-bottom-symmetric $XP_2$ ligand (distinct from those of compound **1**), and the $^{31}$P NMR spectrum features a single peak at –85.14 ppm, which is slightly shifted compared to that of **1**. The reaction to form **2** is reversible, since stirring **2** in DME at room temperature regenerates compound **1**.

The solid-state structure of **2** consists of two $K_2$($XP_2$) units linked to form a $K_4P_4$ cube, with K–P–K and P–K–P angles of 80–90° and 89–101°, respectively (Figure 4). The K–P distances in the square faces bridged by the xanthene backbone lie in a narrow range [3.201(3)–3.249(3) Å], and are shorter than the K–P bonds in **1**. By contrast, the K–P distances linking these two faces are longer, at 3.328(3), 3.335(3), 3.540(3), and 3.568(3) Å; the two shorter K–P bonds are augmented by interactions between potassium and the *ipso*- and *ortho*-carbon atoms of an aryl group on phosphorus [K–C = 3.32(1)–3.40(1) Å; f in Figure 5], whereas the longer K–P bonds are not bridged by comparable K–$C_{aryl}$ interactions (K–C > 3.8 Å). Nevertheless, a similar range of K–P distances was reported for polymeric [{$K_2$(POP)}$_\infty$] [3.220(1)–3.518(1) Å][21] and tetrametallic [{(PNP)$K_2$(THF)$_3$}$_2$] [3.228(1)–3.538(1) Å].[20] The K–$O_{THF}$ distances of 2.667(5)–2.712(6) Å in **2** lie within the typical range.[20,23] By contrast, the K–$O_{xant}$ distances are significantly longer; at 3.033(6)–3.141(6) Å, these bonds are longer than the K–$O_{xant}$ bonds in [$K_2$(XAT)-(alkane)] [XAT = 4,5-bis(2,6-dimesitylanilido)-2,7-di-*tert*-butyl-9,9-dimethylxanthene; 2.534(3)–2.619(2)],[24] $K_2$(POP) [2.869(2) Å], and **1** [2.868(3)–2.958(2) Å].

While a significant number of $Li_4$($NR_2$)$_4$ cubic cage structures have been described,[25] only a handful of cubic $M_4$($PnR_2$)$_4$ cage structures incorporating heavier alkali metal and/or pnictogen elements have been reported. In fact, structurally characterized examples are limited to [{$Li_4$(PH-Si*t*BuAr-PSiPh$_3$)$_2$}$_2$($Li_2Cl_2$)] featuring two $Li_4P_4$ cubes bridged by a $Li_2Cl_2$ unit (a in Figure 5);[26] [{$Na_4$($NMe_2$)$_4$}{(Na(tmeda))$_3$($NMe_2$)$_3$}$_2$] presenting a central $Na_4N_4$ cube linked through opposite faces to $Na_3N_3$ ladder structures; related [{$Na_6$($NMe_2$)$_6$}{(Na(tmeda))$_3$($NMe_2$)$_3$}$_2$] with an $Na_6N_6$ core composed of two face-sharing cubes (b in Figure 5); [{Rb(PH(Dmp))}$_4$]·$C_7H_8$ (Dmp = 2,6-dimesitylphenyl) with a $Rb_4P_4$ core (c in Figure 5);[27] [$Cs_4$(NH(SiMe$_3$)}$_4$] with a $Cs_4N_4$ core (d in Figure 5);[28] and [{Cs(η$^6$-Toluene)}$_4${P(H)Si*t*Bu$_3$}$_4$] with a

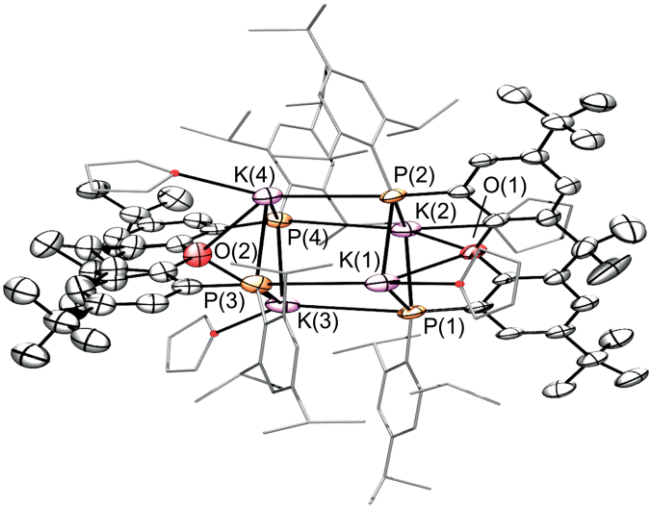


Figure 4. X-ray crystal structure of compound **2**. Ellipsoids are set at 50 % probability. Hydrogen atoms are omitted, and the 2,4,6-triisopropylphenyl groups and coordinated THF molecules are depicted in wire-frame. Interactions between K(1) and the aryl ring on P(3), and K(4) and the aryl ring on P(2) are not shown for clarity. The *tert*-butyl groups are rotationally disordered over multiple positions, and in each case, only one is shown for clarity. Selected bond lengths [Å] and angles [°]: K(1)–P(1) 3.203(3), K(1)–P(2) 3.218(3), K(2)–P(1) 3.201(3), K(2)–P(2) 3.232(3), K(3)–P(3) 3.249(3), K(3)–P(4) 3.217(3), K(4)–P(3) 3.221(3), K(4)–P(4) 3.215(2), K(1)–P(3) 3.328(3), K(2)–P(4) 3.540(3), K(3)–P(1) 3.568(3), K(4)–P(2) 3.335(3), K(1)–O(1) 3.141(6), K(2)–O(1) 3.049(5), K(3)–O(2) 3.033(6), K(4)–O(2) 3.127(5), K(3)–P(4)–K(2) 79.77(6), K(2)–P(1)–K(3) 79.56(6), all other K–P–K = 85.06(7)–90.37(6), P(1)–K(2)–P(4) 100.62(7), P(4)–K(3)–P(1) 99.71(7), all other P–K–P = 88.98(7)–95.66(7).

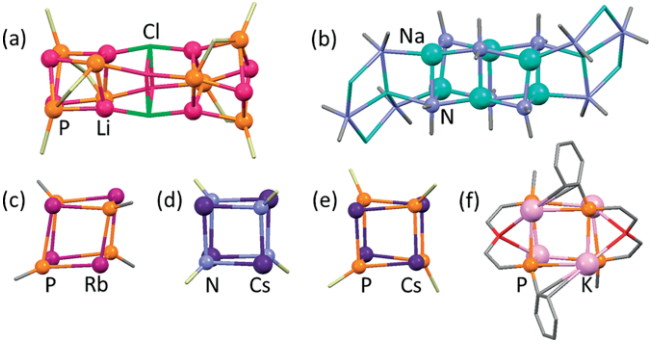


Figure 5. The central cores of (a) [{$Li_4$(PH-Si*t*BuAr-PSiPh$_3$)$_2$}$_2$($Li_2Cl_2$)], (b) [{$Na_6$($NMe_2$)$_6$}{(Na(tmeda))$_3$($NMe_2$)$_3$}$_2$], (c) [{Rb(PH(Dmp))}$_4$]·$C_7H_8$ (Dmp = 2,6-dimesitylphenyl), (d) [$Cs_4$(NH(SiMe$_3$)}$_4$], (e) [{Cs(η$^6$-toluene)}$_4${P(H)Si*t*Bu$_3$}$_4$], and (f) compound **2**. $M_4Pn_4$ cores are shown in ball-and-stick format, while key surrounding atoms (not including H atoms) are shown as capped sticks.

$Cs_4P_4$ core (e in Figure 5).[29] Compound **2** is therefore the first structurally characterized phosphido complex featuring a cubic $K_4P_4$ core.

Reaction of [$K_2$($XP_2$)(dme)$_{2.5}$] with [$YI_3$(THF)$_{3.5}$] in THF produced a mixture of products (consistently >10 peaks in the $^{31}$P NMR spectrum) including [($XP_2$)YI(THF)$_2$] (**3**) and tris(2,4,6-triisopropylphenyl)triphosphirane {(PTripp)$_3$};[30] the latter compound was identified by $^1$H, $^{13}$C and $^{31}$P NMR spectroscopy (comparison with an independently prepared sample) and X-ray crystallography [Figure 6; the structure is closely analogous to

those of $(PMes)_3$[31] and $(PAnt)_2(PAr)$;[32] Mes = mesityl, Ant = 9-Anthracenyl; Ar = $C_6H_2\{o\text{-}CH(SiMe_3)_2\}_2\{p\text{-}C(SiMe_3)_3\}$]. Crude **3** was isolated as the major product after extraction into a small volume of hexanes, and pure **3** was isolated as an orange powder by a second extraction with a small volume of either $O(SiMe_3)_2$ or hexanes in an 18 % overall yield (Scheme 2). X-ray quality crystals were obtained by cooling a concentrated hexanes solution of **3** to −30 °C (Figure 7). It is of note that the unexpected byproducts formed in the synthesis of **3** do not arise from thermal decomposition of **3** over the duration of the reaction, given that the $^{31}P$ NMR signal for **3** did not decrease in intensity once the reaction reached completion.

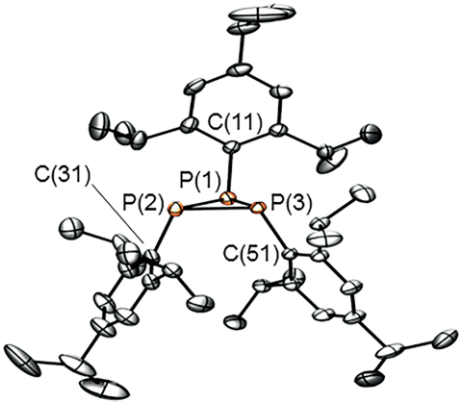


Figure 6. X-ray crystal structure of $(PTripp)_3$ with ellipsoids set to 50 % probability. Hydrogen atoms are omitted for clarity. Selected bond lengths [Å] and angles [°]: P(1)–P(2) 2.2367(6), P(1)–P(3) 2.2060(6), P(2)–P(3) 2.2151(6), P(1)–C(11) 1.864(2), P(2)–C(31) 1.852(2), P(3)–C(51) 1.849(2), P(2)–P(1)–P(3) 59.81(2), P(1)–P(2)–P(3) 59.41(2), P(1)–P(3)–P(2) 60.78(2), C(11)–P(1)–P(2) 101.01(5), C(11)–P(1)–P(3) 96.76(5), C(31)–P(2)–P(1) 107.69(6), C(31)–P(2)–P(3) 112.08(6), C(51)–P(3)–P(1) 115.24(5), C(51)–P(3)–P(2) 116.53(5).

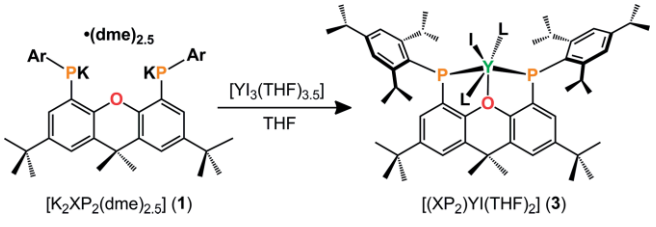


Scheme 2. Attachment of the $XP_2$ ligand to yttrium by salt metathesis (L = THF).

The X-ray crystal structure of **3** (Figure 7) revealed that the xanthene backbone of the $XP_2$ ligand is planar, and the geometry at yttrium is approximately face-capped trigonal bipyramidal with the anionic donors in equatorial positions and the THF ligands in axial positions. Yttrium lies 1.55 Å out of the P(1)/C(4)/C(5)/P(2) plane, leading to an 85° angle between the P(1)/C(4)/C(5)/P(2) plane and the PYP plane. By comparison; yttrium lies 0.50 Å out of the N(1)/C(4)/C(5)/N(2) plane of the related $XN_2$ ligand in $[(XN_2)Y(CH_2SiMe_3)(THF)]$ (Figure 8), with a 31° angle between the N(1)/C(4)/C(5)/N(2) plane and the NYN plane.[6] The P(1)–Y–P(2), P(1)–Y–I, and P(2)–Y–I angles in the equatorial plane of **3** are 110.87(7), 122.43(5) and 121.79(5)°,

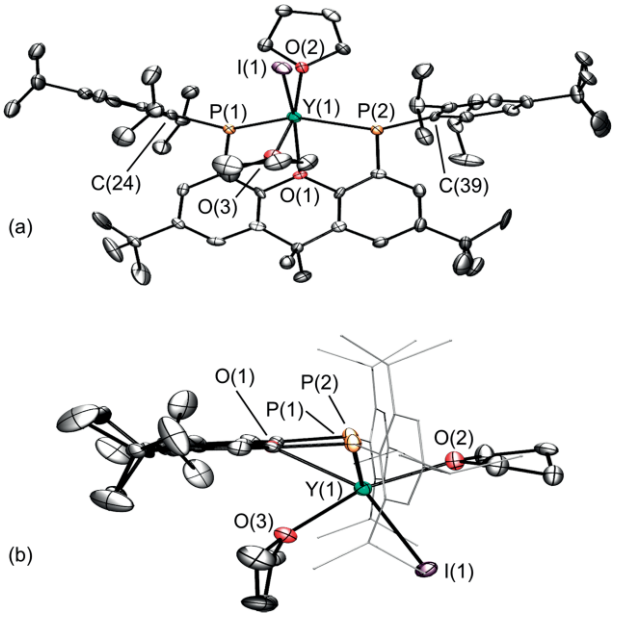


Figure 7. Two views of the X-ray crystal structure of compound **3**. Ellipsoids are set to 50 % probability. Hydrogen atoms are omitted for clarity. The *tert*-butyl groups are rotationally disordered over multiple positions, and in each case, only one is shown for clarity. In view b, the 2,4,6-triisopropylphenyl groups are depicted in wire-frame. Selected bond lengths [Å] and angles [°]: Y–P(1) 2.715(2), Y–P(2) 2.762(2), Y–I 2.9639(10), Y–O(1) 2.508(4), Y–O(2) 2.322(5), Y–O(3) 2.336(5), P(1)–Y–P(2) 110.87(7), P(1)–Y–I 122.43(5), P(2)–Y–I 121.79(5), O(2)–Y–O(3) 162.0(2), O(2)–Y–I 81.6(1), O(3)–Y–I 81.9(1), O(1)–Y–O(2) 126.6(2), O(1)–Y–O(3) 70.3(2), O(1)–Y–P(1) 68.6(1), O(1)–Y–P(2) 67.4(1).

respectively, with an I–Y–[P(1)P(2)centroid] angle of 159.5°. The O(2)–Y–O(3) angle is 162.0(2)°, and the O(2)–Y–I and O(3)–Y–I angles are 81.6(1)° and 81.9(1)°, respectively. The O(1) donor of the xanthene backbone caps the centre of the P(1)/P(2)/O(3) face with O(1)–Y–P and O(1)–Y–O(3) angles between 67.4(1) and 70.3(2)°.

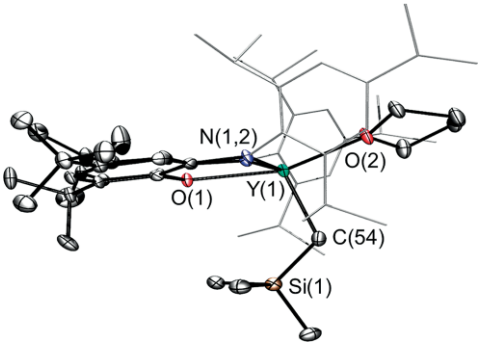


Figure 8. X-ray crystal structure of previously reported $[(XN_2)Y(CH_2SiMe_3)(THF)]$, highlighting the extent to which yttrium lies within the plane of the ligand. Reproduced with permission from reference 6. Copyright 2017 American Chemical Society.

The Y–P distances in **3** are 2.715(2) Å and 2.762(2) Å, falling near the middle of the spectrum observed for the terminal phosphido ligands in $[(Y\{P(SiMe_3)_2\}_2\{\mu\text{-}P(SiMe_3)_2\})_2]$ [2.660(2)–2.693(2) Å],[33] $[Y\{P(SiMe_3)Ar\}I_2(thf)_3]$ (Ar = 2,6-$C_6H_3iPr_2$)

[2.699(2) Å],[34] [$(Cp^{TMS2})_2Y(PHR)(THF)$] [$Cp^{TMS2}$ = 1,3-$C_5H_3(SiMe_3)_2$; R = Si*t*$Bu_3$] [2.770(1) Å],[33] [{($Me_4C_5$-$SiMe_2$-PAr)Y(THF)(μ-H)}$_2$] (Ar = 2,4,6-$C_6H_2$*t*$Bu_3$) [2.724(1) Å], [{$Me_4C_5$-$SiMe_2$–P–$C_6H_2$(2,4-*t*Bu)$_2$(6-$CMe_2CH_2$)}$Y(THF)_2$] [2.789(2) Å], [($Me_4C_5$-$SiMe_2$-PPh)Y(THF)(μ-H)$_2$(μ-PhP-$SiMe_2$–$C_5Me_4$)$Y(THF)_2$] [2.826(2) Å],[16] and [($\kappa^3$-Tp*)(Cp)$Y(PPh_2)(THF)$] [Tp* = tris(3,5-dimethylpyrazolyl)-hydroborate] [2.845(2) Å].[35]

The Y–I distance of 2.964(1) Å in **3** is also within the range previously reported for yttrium iodido compounds. For example, the Y–I distances are 2.9287(3) and 2.9464(3) Å in [{$HC(CMeNAr)_2$}$YI_2(THF)$],[36] 2.947(1)–2.979(1) Å in [Y{$P(SiMe_3)$-Ar}$I_2(thf)_3$] (Ar = 2,6-$C_6H_3$*i*$Pr_2$),[34] and 3.0161(8) Å in [YI{$N(SiMe_3)_2$}$_2(CH_2PPh_3)$].[37] The Y–$O_{THF}$ distances of 2.322(5) and 2.336(5) Å are typical,[36,38] whereas the Y–O(1) distance of 2.508(4) Å is substantially elongated, reflecting the poor donor ability of a diarylether ligand, combined with steric constraints imposed by the rigidity of the $XP_2$ pincer ligand framework.

Between 25 °C and –90 °C, solution $^1$H NMR spectra of **3** in [$D_8$]THF indicate apparent $C_{2v}$ symmetry, consistent with rapid migration of the $YI(THF)_2$ unit from one side of the plane of the ligand backbone to the other. Compound **3** gave rise to a $^{31}$P NMR signal at $\delta$ = 1.28 ppm with a $^1J_{31P,89Y}$ coupling of 162 Hz. This coupling is slightly larger than those observed for the terminal yttrium phosphido complexes [Y{$P(SiMe_3)Ar$}$I_2(thf)_3$] (Ar = $C_6H_3$*i*$Pr_2$-2,6) (157 Hz),[34] [$(Cp^{TMS2})_2Y(PHR)(THF)$] [$Cp^{TMS2}$ = 1,3-$C_5H_3(SiMe_3)_2$; R = Si*t*$Bu_3$] (144 Hz)[33] and [(Y{$P(SiMe_3)_2$}$_2$-{μ-$P(SiMe_3)_2$})$_2$] (122 Hz),[39] and significantly larger than those reported for the aforementioned intact and cyclometallated $Me_4C_5$-$SiMe_2$-PAr complexes (53–84 Hz).[16]

In an attempt to isolate an $XP_2$ yttrium monoalkyl complex, two routes were employed; alkane elimination and salt metathesis. The alkane elimination reaction between [$Y(CH_2SiMe_3)_3(THF)_2$] and $H_2XP_2$ ($C_6D_6$ solvent, 20 °C) yielded only unreacted $H_2XP_2$, and the products of [$Y(CH_2SiMe_3)_3(THF)_2$] thermal decomposition. The salt metathesis reaction between **3** and $NaCH_2SiMe_3$ (1 or 2 equiv. in THF) afforded a major product believed to be [$(XP_2)Y(CH_2SiMe_3)_2(THF)_n]^-$ by $^1$H NMR spectroscopy. However, the reaction was not clean, and despite numerous attempts, this "ate" complex could not be isolated in pure form.

## Conclusions

The rigid POP pincer pro-ligand, $H_2XP_2$, was synthesized in two steps from $XBr_2$. Double deprotonation with excess KH yielded [$K_2XP_2(dme)_n$] (**1**; *n* = 2.5–4) with a rhombus-shaped $K_2P_2$ core, or [$K_4(XP_2)_2(THF)_4$] (**2**) featuring the first cubic $K_4P_4$ cage structure, depending on purification conditions. Reaction of **1** with [$YI_3(THF)_{3.5}$] afforded [$(XP_2)YI(THF)_2$] (**3**) in which Y is displaced 1.55 Å out of the P(1)/C(4)/C(5)/P(2) plane of the $XP_2$ ligand, contrasting the coordination behavior of yttrium to $XN_2$, the amido-analogue of the $XP_2$ dianion. However, the reaction to form **3** is low yielding due to the formation of multiple products including tris(2,4,6-triisopropylphenyl)triphosphirane, {P(Tripp)}$_3$, indicative of poor ligand stability in the presence of strong Lewis acids.

## Experimental Section

**General Details:** An argon-filled MBraun UNIlab glove box equipped with a –30 °C freezer was employed for the manipulation and storage of all air-sensitive compounds, and reactions were performed on a double manifold high vacuum line using standard techniques.[40] A Fisher Scientific Ultrasonic FS-30 bath was used to sonicate reaction mixtures where indicated. A VWR Clinical 200 Large Capacity Centrifuge (with 28° fixed-angle rotors that hold 12 × 15 mL or 6 × 50 mL tubes) in combination with 15 mL Kimble Chase glass centrifuge tubes was used when required (inside the glovebox). Residual oxygen and moisture was removed from the argon stream by passage through an Oxisorb-W scrubber from Matheson Gas Products. Diethyl ether, THF, toluene, benzene and hexanes were initially dried and distilled at atmospheric pressure from $Na/Ph_2CO$. Hexamethyldisiloxane [$O(SiMe_3)_2$] was dried and distilled at atmospheric pressure from Na. Unless otherwise noted, all proteo solvents were stored over an appropriate drying agent {pentane, hexanes, hexamethyldisiloxane [$O(TMS)_2$/$O(SiMe_3)_2$]: $Na/Ph_2CO$/tetra-glyme; $Et_2O$: $Na/Ph_2CO$} and introduced to reactions through vacuum transfer with condensation at –78 °C. The deuterated solvents (ACP Chemicals) $C_6D_6$, [$D_8$]THF and [$D_8$]toluene were dried with $Na/Ph_2CO$.

The 4,5-Dibromo-2,7-di-*tert*-butyl-9,9-dimethylxanthene,[41] [$Y(CH_2SiMe_3)_3(THF)_2$],[42] 2,4,6-triisopropylphenyldichlorophosphine,[43] and $NaCH_2SiMe_3$[44] starting materials were prepared according to literature procedures. 1,3,5-triisopropylbenzene, xanthone, KH (30 wt.-% in mineral oil), $LiCH_2SiMe_3$ (1.0 M in pentane), *n*BuLi (1.6 M in hexanes), $Br_2$, $YI_3$, $YCl_3$, NaO*t*Bu and $LiAlH_4$ were purchased from Sigma–Aldrich. Solid $LiCH_2SiMe_3$ was obtained by removal of pentane in vacuo, and solid KH was obtained by filtration and washing with hexanes. $YI_3(THF)_{3.5}$ and $YCl_3(THF)_{3.5}$ were obtained by refluxing the anhydrous yttrium trihalide in THF for 24 h followed by removal of the solvent in vacuo. Argon (99.999 % purity) and ethylene (99.999 % purity) were purchased from Praxair.

Combustion elemental analyses were performed on a Thermo EA1112 CHNS/O analyzer at McMaster University and by Midwest Microlab, LLC, Indianapolis, Indiana. NMR spectroscopy [$^1$H, $^{13}$C($^1$H), $^{31}$P($^1$H), DEPT-Q, COSY, HSQC, HMBC] was performed on Bruker AV-200, DRX-500 and AV-600 spectrometers. All $^1$H NMR and $^{13}$C NMR spectra were referenced relative to $SiMe_4$ through a resonance of the employed deuterated solvent or proteo impurity of the solvent; $C_6D_6$ ($\delta$ =7.16 ppm), $d_8$-Tol (2.08, 6.97, 7.01, 7.09 ppm), [$D_8$]THF (1.72, 3.58 ppm) for $^1$H NMR; and $C_6D_6$ ($\delta$ =128.0 ppm), $d_8$-Tol (20.43, 125.13, 127.96, 128.87, 137.48 ppm), [$D_8$]THF (25.31, 67.21 ppm) for $^{13}$C NMR spectroscopy. $^{31}$P{$^1$H} NMR spectra were referenced using an external standard of 85 % $H_3PO_4$ in $D_2O$ ($\delta$ =0.0 ppm). Herein, numbered proton and carbon atoms refer to the positions of the xanthene backbone, as shown in Scheme 1. Inequivalent *ortho* isopropyl protons are labeled A and B, so that the corresponding carbon resonances can be identified. X-ray crystallographic analyses were performed on suitable crystals coated in Paratone oil and mounted on a SMART APEX II diffractometer with a 3 kW Sealed tube Mo generator in the McMaster Analytical X-ray (MAX) Diffraction Facility. In all cases, non-hydrogen atoms were refined anisotropically and H atoms were generated in ideal positions and then updated with each cycle of refinement.

CCDC 1544974 (for **1**), 1544974 (for **2**), 1544974 (for **3**), and 1544977 {for [(PTripp)$_3$]} contain the supplementary crystallographic data for this paper. These data can be obtained free of charge from The Cambridge Crystallographic Data Centre.

**$XP_2Cl_2$:** A 1.6 M solution of *n*BuLi in hexanes (12.3 mL, 19.6 mmol) was added to a solution of 4,5-dibromo-2,7-di-*tert*-butyl-9,9-dimeth-

ylxanthene (4.72 g, 9.82 mmol) in THF (120 mL) at –78 °C, and the reaction mixture was stirred at –78 °C for 6 h. A solution of (2,4,6-triisopropylphenyl)dichlorophosphine (6.0 g, 19.6 mmol) in THF (45 mL) was then added, and the reaction mixture and was warmed to room temperature and stirred for 40 h. Solvent was removed in vacuo and the resulting yellow solid was dissolved in toluene (75 mL), centrifuged and the mother liquors were decanted and the solvents evaporated to dryness. To the resulting tacky yellow solid, hexanes (60 mL) was added followed by sonication and solvent removal in vacuo to yield $XP_2Cl_2$ as a free-flowing off-white solid (6.1 g, 73 %). This product is an approximate 1:1 mixture of diastereomers, and was of sufficient purity to proceed to the next step of the ligand synthesis (diastereomers were not identified as *rac* or *meso*, since both diastereomers gave rise to only one $CMe_2$ signal in the $^1H$ and $^{13}C$ NMR spectra, presumably due to overlapping signals in the case of the $C_s$-symmetric *meso* isomer). However, the diastereomers (referred to as A and B) could be separated by sonication in hexanes (4 mL per g of product) followed by centrifugation and separation of the solid from the mother liquors. The solid is > 95 % diastereomer A (isolated in 26 % yield from the crude) while the mother liquors are enriched in diastereomer B (a 3:1 B:A ratio is typical). *NMR spectroscopic data for diastereomer A:* $^1H$ NMR ($C_6D_6$, 600 MHz): $\delta$ = 7.43, 7.15 (s, 2 × 2 H, Xanth-C*H*$^1$ and Xanth-C*H*$^3$), 7.23 (s, 4 H, Ar-*H*), 4.25, 4.26 (sept, $^3J_{H,H}$ = 6.5 Hz, 2 × 2 H, *ortho*-C*H*Me$_2$), 2.76 (sept, $^3J_{H,H}$ = 7.0 Hz, 2 H, *para*-C*H*Me$_2$), 1.45 (s, 6 H, C*Me*$_2$), 1.30, 1.26 (d, $^3J_{H,H}$ = 6.5 Hz, 2 × 12 H, *ortho*-CH*Me*$_2$), 1.20, 1.19 (d, $^3J_{H,H}$ = 7.0 Hz, 2 × 6 H, *para*-CH*Me*$_2$), 1.17 (s, 18 H, C*Me*$_3$) ppm. $^{13}C$ NMR ($C_6D_6$, 126 MHz): $\delta$ = 156.40 (*ortho*-*C*CHMe$_2$), 152.54 (*para*-*C*CHMe$_2$), 150.56 (Xanth-*C*$^{11}$), 144.97 (Xanth-*C*$^2$), 130.64 (d, Ar-*C*$_{ipso}$), 129.83 (Xanth-*C*$^{10}$), 127.81, 125.85 (Xanth-*C*$^1$H and Xanth-*C*$^3$H), 122.94 (Ar-CH), 34.76 (*para*-*C*HMe$_2$), 33.42 (C*Me*$_2$), 32.31, 32.15 (2 × *ortho*-C*H*Me$_2$), 31.42 (C*Me*$_3$), 26.03, 24.40 (2 × *ortho*-CH*Me*$_2$), 24.02, 23.89 (2 × *para*-CH*Me*$_2$) ppm. $^{31}P$ NMR ($C_6D_6$, 243 MHz): $\delta$ = 75.52 ppm. *NMR spectroscopic data for diastereomer B:* $^1H$ NMR ($C_6D_6$, 600 MHz): $\delta$ = 7.55, 7.41 (s, 2 × 2 H, Xanth-C*H*$^1$ and Xanth-C*H*$^3$), 7.24 (s, 4 H, Ar-*H*), 4.31, 4.32 (sept, $^3J_{H,H}$ = 6.7 Hz, 2 × 2 H, *ortho*-C*H*Me$_2$), 2.78 (sept, $^3J_{H,H}$ = 6.8 Hz, 2 H, *para*-C*H*Me$_2$), 1.36 (s, 6 H, C*Me*$_2$), 1.32, 1.27 (d, $^3J_{H,H}$ = 6.7 Hz, 2 × 12 H, *ortho*-CH*Me*$_2$), 1.24 (d, $^3J_{H,H}$ = 6.8 Hz, 12 H, *para*-CH*Me*$_2$), 1.13 (s, 18 H, C*Me*$_3$) ppm. $^{13}C$ NMR ($C_6D_6$, 126 MHz): $\delta$ = 156.38 (*ortho*-*C*CHMe$_2$), 151.25 (Xanth-*C*$^{11}$), 149.15 (*para*-*C*CHMe$_2$), 147.46 (Xanth-*C*$^2$), 131.50 (Xanth-*C*$^{10}$), 130.62 (Ar-*C*$_{ipso}$), 127.83, 124.94 (Xanth-*C*$^1$H and Xanth-*C*$^3$H), 122.80 (Ar-CH), 34.73 (*para*-*C*HMe$_2$), 31.83, 31.60 (2 × *ortho*-*C*HMe$_2$), 31.70 (C*Me*$_2$), 31.49 (C*Me*$_3$), 25.62, 24.99 (2 × *ortho*-CH*Me*$_2$), 24.46, 24.40 (2 × *para*-CH*Me*$_2$) ppm. $^{31}P$ NMR ($C_6D_6$, 243 MHz): $\delta$ = 76.81 ppm. $C_{53}H_{74}Cl_2OP_2$ (860.02): calcd. C 74.01, H 8.67; found C 73.85, H 8.95.

**$H_2XP_2$·*n*LiCl (*n* = 1–1.5):** A solution of $XP_2Cl_2$ (4.0 g, 4.65 mmol) in toluene (60 mL) was added to a solution of $LiAlH_4$ (0.194 g, 5.11 mmol) in diethylether (200 mL) at –78 °C. The reaction mixture was stirred for 2 h before warming to room temperature and stirring for an additional 24 h. The solvent was removed in vacuo followed by centrifugation in toluene (45 mL) and evaporation of the mother liquor to dryness to yield a pale yellow solid. Hexanes (35 mL) was added followed by centrifugation and evaporation of the mother liquor. The resulting white solid was heated under vacuum at 60 °C for 2 d to remove all remaining solvent, yielding $H_2XP_2$·*n*LiCl (*n* = 1–1.5) (3.20 g, 87 %). $^1H$ NMR ($C_6D_6$, 600 MHz): $\delta$ = 7.34, 6.88 (m, 2 × 4 H, Xanth-C*H*$^1$ and Xanth-C*H*$^3$ *rac* and *meso*), 7.27 (s, 8 H, Ar-*H*, *rac* and *meso*), 6.37 (d, $^1J_{H,P}$ = 229 Hz, 2 H, P-*H*), 6.17 (d, $^1J_{H,P}$ = 225 Hz, 2 H, P-*H*), 4.01, 4.00 (2 sept, $^3J_{H,H}$ = 6.5 Hz, 2 × 4 H, *ortho*-C*H*Me$_2$ *rac* and *meso*), 2.83, 2.82 (2 sept, $^3J_{H,H}$ = 7.0 Hz, 2 × 2 H, *para*-C*H*Me$_2$ *rac* and *meso*), 1.54 (s, 6 H, C*Me*$_2$ *rac*), 1.53, 1.51 (s, 2 × 3 H, C*Me*$_2$ *meso*), 1.30, 1.27 (d, $^3J_{H,H}$ = 6.5 Hz, 2 × 12 H, *ortho*-CH*Me*$_2$), 1.25–1.23 (m, 48 H, *ortho*-, *para*-CH*Me*$_2$), 1.17, 1.17 (s, 2 × 18 H, C*Me*$_3$ *rac* and *meso*) ppm. $^{13}C$ NMR ($C_6D_6$, 126 MHz): $\delta$ = 155.43, (*ortho*-*C*CHMe$_2$), 151.12 (*para*-*C*CHMe$_2$), 149.71, 149.31 (Xanth-*C*$^{11}$), 145.98, 145.87 (Xanth-*C*$^2$), 129.36, 128.94 (Xanth-*C*$^{10}$), 127.81, 127.68 (Xanth-*C*$^1$H or Xanth-*C*$^3$H), 122.02, 121.87, 121.71 (Ar-CH, 2 × Xanth-*C*$^1$H or Xanth-*C*$^3$H), 35.26, 35.07, 34.67 (2 × Xanth-*C*$^9$Me$_2$, *C*Me$_3$), 34.94 (*para*-*C*HMe$_2$), 33.49, 31.42 (C*Me*$_2$ *meso*), 33.39, 33.35, 33.31 (*ortho*-*C*HMe$_2$), 32.07 (C*Me*$_2$ *rac*), 31.63 (C*Me*$_3$), 25.43, 25.38 (*ortho*-CH*Me*$_2$), 24.45, 24.43, 24.25, 24.19 (*ortho*-CH*Me*$_2$, *para*-CH*Me*$_2$) ppm. $^{31}P$ NMR ($C_6D_6$, 81 MHz): $\delta$ = –93.07 (d, $^1J_{P,H}$ = 225 Hz), –93.77 (d, $^1J_{P,H}$ = 229 Hz) ppm. $C_{53}H_{76}P_2O$: calcd. C 80.46, H 9.68. Range from duplicate analyses on 4 different batches: C 76.49; H 9.72 to C 74.78, H 8.70. These data correspond to ($C_{53}H_{76}P_2O$)·*n*LiCl (*n* = 1–1.5), since $C_{53}H_{76}P_2OLiCl$ is C 76.36, H 9.19, and $C_{53}H_{76}P_2OLi_{1.5}Cl_{1.5}$ is C 74.47, H 8.96.

**[$K_2$($XP_2$)(DME)$_{2.5}$] (1):** Solid KH (0.126 g, 3.16 mmol) was added to a solution of $H_2[XP_2]$·*n*LiCl (*n* = 1), (1.0 g, 1.20 mmol) in DME (40 mL), and the reaction was stirred at 24 °C for 72 h in the glove box. The orange reaction mixture was filtered, and the filtrate was evaporated to dryness in vacuo. Addition of hexanes (15 mL), centrifugation, and evaporation of the mother liquors to dryness afforded [$K_2$($XP_2$)-(DME)$_{2.5}$] (1.1 g, 80 %) as an orange solid. Crystals of [$K_2$($XP_2$)(DME)$_4$] were grown by cooling a concentrated DME solution to –30 °C. $^1H$ NMR ($C_6D_6$, 600 MHz): $\delta$ = 7.43 (s, 4 H, Ar-*H*), 6.78, 6.65 (s, 2 H, Xanth-C*H*$^1$ and Xanth-C*H*$^3$), 4.54 (sept, $^3J_{H,H}$ = 6.5 Hz, 4 H, *ortho*-C*H*Me$_2$), 3.06 (sept, $^3J_{H,H}$ = 7.0 Hz, 2 H, *para*-C*H*Me$_2$), 2.99 (s, 10 H, 2.5 equiv. DME-CH$_2$), 2.88 (s, 15 H, 2.5 equiv. DME-CH$_3$), 1.86 (s, 6 H, C*Me*$_2$), 1.52 (d, $^3J_{H,H}$ = 6.5 Hz, 12 H, *ortho*-CH*Me*$_2$), 1.45 (d, $^3J_{H,H}$ = 7.0 Hz, 12 H, *para*-CH*Me*$_2$), 1.38 (d, $^3J_{H,H}$ = 6.5 Hz, 12 H, *ortho*-CH*Me*$_2$), 1.30 (s, 18 H, C*Me*$_3$) ppm. $^{13}C$ NMR ($C_6D_6$, 126 MHz): $\delta$ = 155.16 (*ortho*-*C*CHMe$_2$), 146.78 (*para*-*C*CHMe$_2$), 144.70 (Xanth-*C*$^{11}$), 144.27 (Xanth-*C*$^2$), 141.18 (Ar-*C*$_{ipso}$), 126.34 (Xanth-*C*$^{10}$), 123.75, 110.69 (Xanth-*C*$^1$H and Xanth-*C*$^3$H), 120.69 (Ar-CH), 71.46 (DME-CH$_2$), 58.49 (DME-CH$_3$), 35.12 (*para*-*C*HMe$_2$), 34.61 (Xanth-*C*$^9$Me$_2$ and/or *C*Me$_3$), 34.16 (C*Me*$_2$), 33.73 (*ortho*-*C*HMe$_2$), 31.96 (C*Me*$_3$), 26.07, 25.00 (2 × *ortho*-CH*Me*$_2$), 24.72 (*para*-CH*Me*$_2$) ppm. $^{31}P$ NMR ($C_6D_6$, 81 MHz): $\delta$ = –83.73 ppm. $C_{63}H_{99}K_2O_6P_2$ (1092.62): calcd. C 69.25, H 9.13; found C 69.69, H 8.98.

**[$K_4$($XP_2$)$_2$(THF)$_4$] (2):** [$K_2$($XP_2$)(dme)$_{2.5}$] (**1**) (95 mg, 0.087 mmol) was dissolved in THF (12 mL) and stirred at 24 °C for 5 h, followed by removal of solvent in vacuo. The resulting amber colored solid was recrystallized from hexanes (1.5 mL) to yield [$K_4$($XP_2$)$_2$(THF)$_4$] (38 mg, 21.6 %) as red-orange crystals. $^1H$ NMR ($C_6D_6$, 600 MHz): $\delta$ = 7.43 (s, 8 H, Ar-*H*), 6.87 (d, $^4J_{H,H}$ = 2.29 Hz, 4 H, Xanth-C*H*$^1$), 6.61 (broad s, 4 H, Xanth-C*H*$^3$), 4.37 (sept, $^3J_{H,H}$ = 7.01 Hz, 8 H, *ortho*-C*H*Me$_2$), 3.55 (m, 16 H, 4 equiv. THF-C$^{2,5}$H$_2$), 3.07 (sept, $^3J_{H,H}$ = 7.01 Hz, 4 H, *para*-C*H*Me$_2$), 1.88 (s, 12 H, C*Me*$_2$), 1.50 (d, $^3J_{H,H}$ = 6.99 Hz, 24 H, **A**-*ortho*-CH*Me*$_2$), 1.46 (d, $^3J_{H,H}$ = 7.02 Hz, 24 H, *para*-CH*Me*$_2$), 1.41 (m, 16 H, 4 equiv. THF-C$^{3,4}$H$_2$), 1.34 (d, $^3J_{H,H}$ = 6.99 Hz, 24 H, **B**-*ortho*-CH*Me*$_2$), 1.33 (s, 36 H, C*Me*$_3$) ppm. $^{13}C$ NMR ($C_6D_6$, 126 MHz): $\delta$ = 154.99 (*ortho*-*C*CHMe$_2$), 147.06 (*para*-*C*CHMe$_2$), 144.57 (Xanth-*C*$^2$), 126.98 (Xanth-*C*$^{10}$), 124.07 (Xanth-*C*$^3$H), 120.80 (Ar-CH), 110.75 (Xanth-*C*$^1$H), 67.82 (THF-C$^{2,5}$H$_2$), 35.12 (*para*-*C*HMe$_2$), 34.83 (Xanth-*C*$^9$Me$_2$), 34.66 (*C*Me$_3$), 33.69 (*ortho*-*C*HMe$_2$), 33.54 (C*Me*$_2$), 31.95 (C*Me*$_3$), 25.94 (**B**-*ortho*-CH*Me*$_2$), 25.80 (THF-C$^{3,4}$H$_2$), 25.04 (**A**-*ortho*-CH*Me*$_2$), 24.69 (*para*-CH*Me*$_2$) ppm. $^{31}P$ NMR ($C_6D_6$, 81 MHz): $\delta$ = –85.14 ppm. $C_{122}H_{180}K_4O_6P_4$ (2023.05): calcd. C 72.43, H 8.97; found C 72.38, H 8.75.

**[($XP_2$)YI(THF)$_2$] (3) and (PTripp)$_3$:** [$K_2$($XP_2$)(dme)$_{2.5}$] (**1**) (0.250 g, 0.228 mmol) and [$YI_3$(THF)$_{3.5}$] (0.166 g, 0.228 mmol) were stirred in THF (25 mL) for 72 h at 24 °C. The bright yellow solution was filtered and the solvent was removed in vacuo. The resulting yellow solid was slurried in hexanes (8 mL) before the mixture was centrifuged

and the mother liquors were evaporated to dryness to provided impure [(XP$_2$)YI(THF)$_2$] (**3**; 0.110 g) as an orange solid. 5 mL of O(SiMe$_3$)$_2$ was added to the impure solid followed by centrifugation. The resulting solid was isolated and dried in vacuo yielding pure [(XP$_2$)YI(THF)$_2$] (0.048 g, 18 % yield). The remaining mother liquors contain a mixture of products, including (PTripp)$_3$, and X-ray quality crystals of (PTripp)$_3$ were obtained by cooling a concentrated hexanes solution of this mixture to –30 °C. X-ray quality crystals of **3** were grown by cooling a concentrated hexanes solution of **3** to –30 °C. Solid samples of [(XP$_2$)YI(THF)$_2$] were observed to lose THF slowly under dynamic vacuum, and the sample used for NMR spectroscopic characterization contained just 1.5 equiv. of THF. $^1$H NMR ([D$_8$]THF, 600 MHz): $\delta$ = 7.11 (s, 4 H, Ar-*H*), 6.74 (d, $^4J_{H,H}$ = 2.0 Hz, 2 H, Xanth-C*H*$^1$), 5.94 (dd, $^4J_{H,H}$ = 2.0, $^3J_{P,H}$ = 8.0 Hz, 2 H, Xanth-C*H*$^3$), 4.40 (sept, $^3J_{H,H}$ = 7.0 Hz, 4 H, *ortho*-C*H*Me$_2$), 3.62 (m, 6 H, 1.5 equiv. THF-C$^{2,5}H_2$), 2.92 (sept, $^3J_{H,H}$ = 7.0 Hz, 2 H, *para*-C*H*Me$_2$), 1.77 (m, 6 H, 1.5 equiv. THF-C$^{3,4}H_2$), 1.54 (s, 6 H, C*Me*$_2$), 1.28 (d, $^3J_{H,H}$ = 7.0 Hz, 12 H, *para*-CH*Me*$_2$), 1.24 (d, $^3J_{H,H}$ = 7.0 Hz, 12 H, **A**-*ortho*-CH*Me*$_2$), 1.01 (d, $^3J_{H,H}$ = 7.0 Hz, 12 H, **B**-*ortho*-CH*Me*$_2$), 0.99 (s, 18 H, C*Me*$_3$) ppm. $^{13}$C NMR ([D$_8$]THF, 126 MHz): $\delta$ = 155.69 (*ortho*-*C*CHMe$_2$), 149.28 (*para*-*C*CHMe$_2$), 144.06 (Xanth-*C*$^2$), 136.51 (d, Ar-*C*$_{ipso}$), 128.02 (Xanth-*C*$^{10}$), 123.94 (Xanth-*C*$^3$H), 121.66 (Ar-*C*H), 114.83 (Xanth-*C*$^1$H), 35.24 (*para*-*C*HMe$_2$), 34.66 (*C*Me$_3$), 34.53 (*ortho*-*C*HMe$_2$), 34.45 (Xanth-*C*$^9$Me$_2$), 33.11 (*C*Me$_2$), 31.49 (*C*Me$_3$), 26.18 (**B**-*ortho*-CH*Me*$_2$), 25.66 (**A**-*ortho*-CH*Me*$_2$), 24.34 (*para*-CH*Me*$_2$) ppm. $^{31}$P NMR ([D$_8$]THF, 81 MHz): $\delta$ = 1.28 (d, $^1J_{Y,P}$ = 162 Hz) ppm. $C_{61}H_{90}IO_3P_2Y$ (1149.14): calcd. C 63.76, H 7.89; found C 60.56, H 7.95. (This compound is extremely air, moisture and temperature sensitive, and some decomposition may have occurred during transport to Indianapolis for elemental analysis).

## Acknowledgments

D. J. H. E. thanks Natural Sciences and Engineering Research Council of Canada (NSERC) for a Discovery Grant and an Strategic Grant in collaboration with NOVA Chemicals. K. S. A. M. thanks the Government of Ontario for an OGS – Queen Elizabeth II Graduate Scholarship in Science and Technology (QEII GSST) scholarship.

**Keywords:** Cage compounds · Phosphido ligand · Pincer ligand · Potassium · Yttrium

[1] C. A. Cruz, D. J. H. Emslie, L. E. Harrington, J. F. Britten, C. M. Robertson, *Organometallics* **2007**, *26*, 692–701.
[2] B. Vidjayacoumar, S. Ilango, M. J. Ray, T. Chu, K. B. Kolpin, N. R. Andreychuk, C. A. Cruz, D. J. H. Emslie, H. A. Jenkins, J. F. Britten, *J. Chem. Soc., Dalton Trans.* **2012**, *41*, 8175–8189.
[3] C. A. Cruz, D. J. H. Emslie, L. E. Harrington, J. F. Britten, *Organometallics* **2008**, *27*, 15–17.
[4] N. R. Andreychuk, S. Ilango, B. Vidjayacoumar, D. J. H. Emslie, H. A. Jenkins, *Organometallics* **2013**, *32*, 1466–1474.
[5] C. A. Cruz, D. J. H. Emslie, C. M. Robertson, L. E. Harrington, H. A. Jenkins, J. F. Britten, *Organometallics* **2009**, *28*, 1891–1899.
[6] K. S. A. Motolko, D. J. H. Emslie, H. A. Jenkins, *Organometallics* **2017**, *36*, 1601–1608.
[7] K. S. A. Motolko, D. J. H. Emslie, J. F. Britten, *RSC Adv.* **2017**, *7*, 27938–27945.
[8] T. S. Li, S. Kaercher, P. W. Roesky, *Chem. Soc. Rev.* **2014**, *43*, 42–57.
[9] K. Izod, P. O'Shaughnessy, J. M. Sheffield, W. Clegg, S. T. Liddle, *Inorg. Chem.* **2000**, *39*, 4741–4748.
[10] a) S. Blair, K. Izod, W. Clegg, *J. Organomet. Chem.* **2003**, *688*, 92–99; b) K. Izod, S. T. Liddle, W. Clegg, R. W. Harrington, *Dalton Trans.* **2006**, 3431–3437.
[11] K. Izod, S. T. Liddle, W. McFarlane, W. Clegg, *Organometallics* **2004**, *23*, 2734–2743.
[12] W. Clegg, K. Izod, S. T. Liddle, P. O'Shaughnessy, J. M. Sheffield, *Organometallics* **2000**, *19*, 2090–2096.
[13] M. Mazzeo, M. Lamberti, I. D'Auria, S. Milione, J. C. Peters, C. Pellecchia, *J. Polym. Sci., Part A J. Polym. Sci. Pol. Chem.* **2010**, *48*, 1374–1382.
[14] H. C. Aspinall, S. R. Moore, A. K. Smith, *J. Chem. Soc., Dalton Trans.* **1993**, 993–996.
[15] O. Tardif, Z. M. Hou, M. Nishiura, T. Koizumi, Y. Wakatsuki, *Organometallics* **2001**, *20*, 4565–4573.
[16] O. Tardif, M. Nishiura, Z. M. Hou, *Tetrahedron* **2003**, *59*, 10525–10539.
[17] K. Izod, S. T. Liddle, W. Clegg, *Chem. Commun.* **2004**, 1748–1749.
[18] V. D. Bianco, S. Doronzo, *Inorg. Synth.* **1976**, *16*, 161.
[19] J. S. Ritch, D. Julienne, S. R. Rybchinski, K. S. Brockman, K. R. D. Johnson, P. G. Hayes, *Dalton Trans.* **2014**, *43*, 267–276.
[20] M. S. Winston, J. E. Bercaw, *Organometallics* **2010**, *29*, 6408–6416.
[21] L. Turculet, R. McDonald, *Organometallics* **2007**, *26*, 6821–6826.
[22] K. Izod, J. Stewart, E. R. Clark, W. Clegg, R. W. Harrington, *Inorg. Chem.* **2010**, *49*, 4698–4707.
[23] a) C. D. Carmichael, M. D. Fryzuk, *Can. J. Chem.* **2010**, *88*, 667–675; b) Y. N. Chang, L. C. Liang, *Inorg. Chim. Acta* **2007**, *360*, 136–142.
[24] N. R. Andreychuk, D. J. H. Emslie, *Angew. Chem. Int. Ed.* **2013**, *52*, 1696–1699; *Angew. Chem.* **2013**, *125*, 1740.
[25] a) D. J. Brauer, H. Burger, G. R. Liewald, *J. Organomet. Chem.* **1986**, *308*, 119–130; b) M. G. Gardiner, C. L. Raston, *Inorg. Chem.* **1996**, *35*, 4047–4059; c) J. K. Brask, T. Chivers, G. Schatte, *Chem. Commun.* **2000**, 1805–1806; d) S. Daniele, C. Drost, B. Gehrhus, S. M. Hawkins, P. B. Hitchcock, M. F. Lappert, P. G. Merle, S. G. Bott, *J. Chem. Soc., Dalton Trans.* **2001**, 3179–3188; e) E. Gellermann, U. Klingebiel, T. Pape, F. D. Antonia, T. R. Schneider, S. Schmatz, *Z. Anorg. Allg. Chem.* **2001**, *627*, 2581–2588; f) J. F. Li, L. H. Weng, X. H. Wei, D. S. Liu, *J. Chem. Soc., Dalton Trans.* **2002**, 1401–1405; g) T. Chivers, C. Fedorchuk, G. Schatte, J. K. Brask, *Can. J. Chem.* **2002**, *80*, 821–831; h) J. S. Hao, X. H. Wei, S. P. Huang, J. P. Guo, D. S. Liu, *Appl. Organomet. Chem.* **2005**, *19*, 1010–1014; i) J. S. M. Lehn, S. Javed, D. M. Hoffman, *Inorg. Chem.* **2007**, *46*, 993–1000; j) A. M. Corrente, T. Chivers, *Inorg. Chem.* **2008**, *47*, 10073–10080.
[26] M. Driess, G. Huttner, N. Knopf, H. Pritzkow, L. Zsolnai, *Angew. Chem. Int. Ed. Engl.* **1995**, *34*, 316–318; *Angew. Chem.* **1995**, *107*, 354.
[27] G. W. Rabe, S. Kheradmandan, G. P. A. Yap, *Inorg. Chem.* **1998**, *37*, 6541–6543.
[28] K. F. Tesh, B. D. Jones, T. P. Hanusa, J. C. Huffman, *J. Am. Chem. Soc.* **1992**, *114*, 6590–6591.
[29] M. Westerhausen, S. Weinrich, B. Schmid, S. Schneiderbauer, M. Suter, H. Noth, H. Piotrowski, *Z. Anorg. Allg. Chem.* **2003**, *629*, 625–633.
[30] a) C. N. Smit, T. A. Vanderknaap, F. Bickelhaupt, *Tetrahedron Lett.* **1983**, *24*, 2031–2034; b) L. Weber, D. Bungardt, R. Boese, D. Bläser, *Chem. Ber.* **1988**, *121*, 1033–1038.
[31] C. Frenzel, E. Hey-Hawkins, *Phosphorus Sulfur Silicon Relat. Elem.* **1998**, *143*, 1–17.
[32] N. Tokitoh, A. Tsurusaki, T. Sasamori, *Phosphorus Sulfur Silicon Relat. Elem.* **2009**, *184*, 979–986.
[33] M. Westerhausen, S. Schniederbauer, M. Hartmann, M. Warchhold, H. Nöth, *Z. Anorg. Allg. Chem.* **2002**, *628*, 330–332.
[34] Y. D. Lv, X. Xu, Y. F. Chen, X. B. Leng, M. V. Borzov, *Angew. Chem. Int. Ed.* **2011**, *50*, 11227–11229; *Angew. Chem.* **2011**, *123*, 11423.
[35] W. Y. Yi, J. Zhang, L. C. Hong, Z. X. Chen, X. G. Zhou, *Organometallics* **2011**, *30*, 5809–5814.
[36] S. T. Liddle, P. L. Arnold, *Dalton Trans.* **2007**, 3305–3313.
[37] M. R. Crimmin, A. J. P. White, *Chem. Commun.* **2012**, *48*, 1745–1747.
[38] S. Krieck, H. Gorls, M. Westerhausen, *Inorg. Chem. Commun.* **2009**, *12*, 409–411.
[39] M. Westerhausen, M. Hartmann, W. Schwarz, *Inorg. Chim. Acta* **1998**, *269*, 91–100.
[40] B. J. Burger, J. E. Bercaw, *Vacuum Line Techniques for Handling Air-Sensitive Organometallic Compounds*. In Experimental Organometallic Chemistry: A Practicum in Synthesis and Characterization (Eds.: A. L. Wayda, M. Y. Dar-

 

ensbourg); ACS Symp. Ser.; American Chemical Society: Washington D. C., **1987**, vol. 357, pp. 79–98.

[41] J. S. Nowick, P. Ballester, F. Ebmeyer, J. J. Rebek, *J. Am. Chem. Soc.* **1990**, *112*, 8902–8906.

[42] F. Estler, G. Eickerling, E. Herdtweck, R. Anwander, *Organometallics* **2003**, *22*, 1212–1222.

[43] a) V. Chandrasekhar, P. Sasikumar, R. Boomishankar, G. Anantharamian, *Inorg. Chem.* **2006**, *45*, 3344–3351; b) G. M. Whitesides, M. Eisenhut, W. M. Bunting, *J. Am. Chem. Soc.* **1974**, *96*, 5398.

[44] E. M. Matson, W. P. Forrest, P. E. Fanwick, S. C. Bart, *Organometallics* **2012**, *31*, 4467–4473.

Received: April 20, 2017